(1)

AD-A284 458

Annual Report of the Research grant

No: N00014-92-J-6003

for the period

September 93 - August 94

funded by the Department of Navy

Principal Investigator: Prof. Sitharama Iyengar

Chairman, Department of Computer Science

Louisiana State University

Baton Rouge, LA 70803.

Previous research

Our research in the past year focused on the design and development of Histogram-Based Morphological Edge Detector (HMED) to extract edges from the infrared images obtained from the Advanced Very High Resolution Radiometer (AVHRR).

The motivation of this research stems from our previous experiences with the edge detectors. For instance, The conventional edge detectors are very sensitive to edge fine structure which makes it difficult to distinguish the weak gradients that are useful in this application from noise.

Image analysis techniques use the histogram for operations such as thresholding and edge extraction in a local neighborhood in the image. The histogram is a popular tool used in image processing and image analysis. It is used for edge detection, thresholding, texture feature extraction and other related problems.

Mathematical morphology has been used in the past to develop efficient and statistically robust edge detectors. Morphological edge detectors are designed to work only in the image domain. Such designs ignore the vital information contained in the histogram of an (sub)image. As a consequence, various weak gradient values pertaining to important features are missed in oceanographic IR images.

This led us to design and develop a morphological edge detector that incorporates information from the image histogram to improve the performance while being conceptually simple and computationally efficient. In doing so, new morphological operations are defined in the domain of the histogram of an image.

We compared our HMED with two other morphological edge detectors, namely Blur-minimization Edge Detector (BMM) and Alph-trimmed Edge Detector (ATM). In the comparison, we concluded that HMED performed better than BMM and ATM.

Current Research

Registration of Synthetic Aperture Radar (SAR) images is performed using the statistical correlation between the two images or minimizing the average fluctuation of the phase difference images.

Images from two satellite passes is registered by computing statistical correlation function between the two images over discrete pixel offsets, then interpolating the correlation function to find its minimum position.

Hybrid Approach: The average fluctuation function is evaluated using values of all pixels at every range and azimuth offsets. We believe that such intensive evaluation is not required.

We are currently investigating an alternative procedure that would select sub-images within the SAR images. The phase difference between the two sub-images is evaluated for each offset. For each subimage the offsets pertaining to the minimum average fluctuation are selected. The sub-images are in fact marked as control points for registration. For each offsets, the global average fluctuation is computed. The final range and azimuth offsets pertaining to the minimum global average fluctuation is computed.

References

[1] Krishnamurthy. S., S. S. Iyengar, R. Holyer and M. Lybanon, "Histogram-Based Morphological Edge Detector," **IEEE Transactions on Geoscience and Remote Sensing**, 32, No 4, 759-767, July, 1994.

[2] Krishnamurthy. S., S. S. Iyengar, R. Holyer and M. Lybanon, "Topography-based Feature labeling for IR oceanographic images," **Pattern Recognition Letters**, 14, pp. 915-925, Nov 1993.

[3] Krishnamurthy. S., S. S. Iyengar, R. Holyer and M. Lybanon, "Morphological Edge Detection in Infrared Oceanographic Images," *in the Proceedings of the SPIE : 22nd AIPR Workshop* , Vol 2103, pp 2-13, 1993.

IEEE TRANSACTIONS ON GEOSCIENCE AND REMOTE SENSING, VOL. 32, NO. 4, JULY 1994

Histogram-Based orphological Edge Detector

Sankar Krishnamurthy, S. Sitharama Iyengar, *Senior Member, IEEE*, Ronald J. Holyer, and Matthew Lybanon

Abstract—We present a new edge detector for automatic extraction of oceanographic (mesoscale) features present in infrared (IR) images obtained from the Advanced Very High Resolution Radiometer (AVHRR). Conventional edge detectors are very sensitive to edge fine structure, which makes it difficult to distinguish the weak gradients that are useful in this application from noise. Mathematical morphology has been used in the past to develop efficient and statistically robust edge detectors. Image analysis techniques use the histogram for operations such as thresholding and edge extraction in a local neighborhood in the image. An efficient computational framework is discussed for extraction of mesoscale features present in IR images. The technique presented here, the *Histogram-Based Morphological Edge detector (HMED)*, extracts all the weak gradients, yet retains the edge sharpness in the image. We also present new morphological operations defined in the domain of the histogram of an image. We provide interesting experimental results from applying the HMED technique to oceanographic data in which certain features are known to have edge gradients of varying strength.

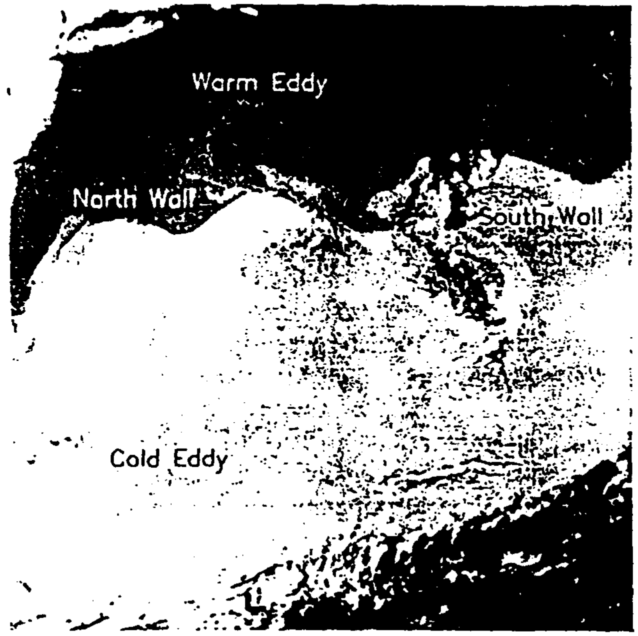

Fig. 1. North Atlantic image obtained on April 17.

I. Introduction

An infrared (IR) image of the ocean obtained from the Advanced Very High Resolution Radiometer (AVHRR) aboard the NOAA-7 satellite is shown in Fig. 1. Such images are widely used for the study of ocean dynamics. In this image, bright areas represent warmer temperatures and light areas represent colder temperatures. The Gulf Stream, cold eddies, and warm eddies (the former are normally found south of the Gulf Stream and the latter north of the Gulf Stream) are examples of "mesoscale" ocean features with dimensions on the order of 50-300 km.

The Gulf Stream is warmer than the Surgasso Sea to its south, and much warmer than the waters to its north. Thus, its northern boundaries are more easily detectable than its southern boundaries in satellite IR images. Sometimes, clouds obscure oceanographic features, making their detection difficult. The movement of these features compounds the problems associated with the detection. For instance, the Gulf Stream can meander 30 km in one day. Sometimes, these meanders lead to the "birth" of a Gulf Stream ring, which is a special type of eddy that forms from a cutoff Gulf Stream meander [1]-[3]. When the Gulf Stream closes on itself, surrounding a mass of cold water at its southern boundary, a counterclockwise-rotating cold ring forms. Similarly, when the Gulf Stream surrounds a mass of warm water at its northern boundary, a clockwise-rotating warm ring originates [4].

Since satellite IR images of the ocean often depict the mesoscale features clearly, AVHRR imagery is used extensively to study them. In Section II, we discuss some techniques developed for the detection of edges in oceanographic images. In Section III, we present recently developed morphological edge detectors, and explain some preliminary concepts of morphological operations. We are not aware of any other morphological edge detectors based on the histogram of an image in the field of image analysis and computer vision. The Histogram-Based Morphological Edge detector (HMED) with the new morphological operations is explained in Section IV. Our implementation's results, when applied to oceanographic images, are given in Section V.

II. Edge Detection in Oceanographic Images

The Naval Research Laboratory began development of the Semi-Automated Mesoscale Analysis System (SAMAS), a comprehensive set of algorithms that handles the entire automated analysis problem, from low-level segmentation through intermediate-level feature formation

Manuscript received October 13, 1993; revised March 31, 1994. This work was supported by the Department of the Navy under Contract N00014-92-J-6003.

S. Krishnamurthy and S. S. Iyengar are with the Department of Computer Science, Louisiana State University, Baton Rouge, LA 70803.

R. J. Holyer and M. Lybanon are with the Remote Sensing Branch, Naval Research Laboratory, Stennis Space Center, MS 39529.

IEEE Log Number 9402675.

and into higher level artificial intelligence modules that estimate positions of previously detected features when cloud cover obscures direct observation in the current image set [5].

The current version of SAMAS groups various modules into these three categories. A cloud detection algorithm processes the thermal infrared image of the ocean to classify all pixels either as cloud pixels or noncloud pixels [6]. Considering only noncloud pixels, the system uses the cluster shade texture measure as the low-level operation and detection of zero crossings in cluster shade as the medium-level operation, leading to a set of edge primitives [7]. SAMAS uses two-step nonlinear relaxation [8] to label edge primitives [9]. In the first relaxation labeling step, *a priori* probability values of the edge pixels are computed using *a priori* knowledge of the approximate sizes and positions of the features, based on a previous analysis (typically from one week earlier). In the second step, these probability values are updated using compatibility coefficients in an iterative fashion, until the values stabilize. The relaxation labeling technique reduces uncertainty in the assignment of labels to edge pixels [9]. We also developed a topographic-based feature labeling module that uses the surface topology of a pixel and its neighborhood [10]. A rule-based expert system predicts the future position of the mesoscale features [5], [11]. We briefly discuss some edge detection algorithms specifically designed for oceanographic images.

SAMAS currently uses a cluster shade algorithm for the detection of edges [7], [12]. The algorithm works in three stages: 1) computation of cluster shade texture measure from the gray-level cooccurrence (GLC matrix), 2) computations of zero crossings in the cluster shade image to detect the edges, and 3) a cleaning/dilation/thining step is applied to the edge image. The cluster shade edge detector is characterized by accurate edge localization while rejecting fine structure within the detected edges.

Cayula and Cornillon [13] have developed an edge-detection algorithm for oceanographic satellite images. Their algorithm operates at three levels: picture level, window level, and local/pixel level. At the picture level, most obvious clouds are identified and tagged so that they do not participate at the lower levels. The cloud-finding procedure is based on temperature and shape. At the window level, the temperature distribution in each window is analyzed to determine the statistical relevance of each possible front, using unsupervised learning techniques. Finally, local edge operators are used to complete the contours found by the region-based algorithm. Since the local operations are used along with the window-based algorithm, the qualities of scale invariance and adaptivity associated with the region-based approach are not lost.

III. Morphological Edge Detectors

Mathematical morphology based on geometric shape is used in biomedical image processing, robot vision systems, and low-level vision problems for its conceptual simplicity. Many techniques in computer vision use mathematical morphology as a tool for the extraction of features and recognition of objects. Matheron [14] introduced the application of mathematical morphology for analyzing the geometric structure of metallic and geologic samples. Serra [15] applied mathematical morphology for image analysis. Haralick [16] presented a review of mathematical morphology applied to image analysis.

Peleg and Rosenfeld [17] use gray-scale morphology to generalize the medial axis transform to gray-scale imaging. Pelag *et al.* [18] measure changes in texture properties as a function of resolution using gray-scale morphology. Werman and Pelag [19] use gray-scale morphology for texture feature extraction. We will study the use of gray-scale morphology and texture information for edge detection in oceanographic images.

Recently, mathematical morphology has been applied for the extraction of edges. Most of the template-based edge detectors are known to perform satisfactorily under high signal-to-noise ratio, but degrade significantly when noise is introduced into the system. Some of the template-based edge detectors are the Prewitt operators and the Kirsh operator. A number of edge detectors fit a polynomial function on the image data. Then, the first and second directional derivatives are computed, from which the edges are extracted. Mathematical morphology-based edge detectors have been shown to outperform most spatial and differentiation-based edge detectors [20]. Morphological edge detectors are local neighborhood nonlinear operators. Appropriately used, morphological techniques tend to simplify image data while preserving the shape characteristics and eliminating irrelevancies. These algorithms often generate useful and surprising results. We briefly present preliminary concepts of mathematical morphology. Matheron [14] gives a detailed discussion of mathematical morphology.

A. Preliminary Concepts

An image "f" is a set of pixels in a rectangular array (mesh). $f(i, j)$ is a pixel at coordinate (i, j) in the image f. A structuring element is analogous to the kernel/template of a convolution operation, and it is associated with a predesigned shape. A structuring element may have any shape. Morphologic operators can be visualized as working with two images, the original image and the structuring element. The structuring element is used as a tool to manipulate the image using various operations, namely, *dilation*, *erosion*, *opening*, and *closing*. The dilation of a binary image f by a structuring element S is defined as

$$f \oplus S = \{a + b | a \in f \wedge b \in S\}.$$

The erosion of a binary image f by a structuring element S is defined as

$$f \ominus S = \{a - b | a \in f \wedge b \in S\}.$$

The "*dilation*" d of a gray-scale image f by a structuring element S is defined as

$$d(i, j) = \text{MAX } (f(i + x, j + y) \oplus S(x, y))$$

where x and y are the coordinates of a cell in S whose center cell is the origin, and $(i + x, j + y)$ is in the domain of f. Similarly, "erosion" of a gray-scale image f by a structuring element S is defined as

$$e(i, j) = \text{MIN}\ (f(i + x, j + y) \ominus S(x, y)).$$

The *closing* operation is a dilation followed by an erosion, and similarly *opening* is an erosion followed by a dilation. Thus, closing is defined as

$$c(i, j) = \text{MIN}\ (d(i + x, j + y) \ominus S(x, y))$$

where d is the dilated image of original image f. Opening is defined as

$$o(i, j) = \text{MAX}\ (e(i + x, j + y) \oplus S(x, y))$$

where e is the eroded image of original image f. A sequence of these gray-scale morphological operations on an image often produces useful results. For instance, a simple morphological edge detector is the *dilation residual* edge image, defined as

$$\text{DR}\ (i, j) = d(i, j) - f(i, j).$$

Similarly, the *erosion residual* edge detector is given by

$$\text{ER}\ (i, j) = f(i, j) - e(i, j).$$

Even though these edge detectors are simple and robust, they are not reliable for extremely noisy images, and introduce spurious edges.

Lee *et al.* [20] designed a Blur-Minimization Morphological (BMM) operator for edge detection. The BMM operator blurs the original image by averaging the pixel values spanned by the structuring element. Dilated and eroded images are generated from the blurred image. Dilation residual and eroded residual images are created using these images. The edge strength at coordinate (i, j) is given by the minimum of the dilation residual and erosion residual. Symbolically, we write

$$\text{BMM}\ (i, j) = \text{MIN}\ (f_a(i, j) - e(i, j), d(i, j) - f_a(i, j))$$

where $f_a = \Sigma f(i + x, j + y)/N$ is the blurred image, N is the number of cells in the structuring element, and $(i + x, j + y)$ is defined in the domain of the image. In spite of being conceptually simple and computationally efficient, the BMM edge detector has been proven to perform better than the spatial- and differential-based edge detectors.

Feehs and Arce [21] showed the importance of blurring the original image for morphological edge detection. They introduced an *Alpha-Trimmed Multidimensional Morphological* (ATM) edge detector that incorporates the opening and closing operations. They also proved statistically that ATM performs better than BMM. Let us consider the ATM edge detector for two-dimensional images with a structuring element of size $n \times n$. The original image is initially blurred by $f_a = \Sigma_{i=\alpha+1}^{k-a} f_i/k - 2 * \alpha$ where $k = n^2$ is the number of pixels in the original image spanned by the structuring image, f_i is the ith smallest valued pixel in the sorted sequence of pixels in f spanned by the structuring element, and α is the trimming factor. If α is 0, we consider all pixels spanned by the structuring element for blurring. If $\alpha = i$, we consider all sorted pixels greater than f_i and less than f_{k-i} spanned by the structuring element. The edge strength at (i, j) computed by the ATM edge detector is

$$\text{ATM}\ (i, j) = \text{MIN}\ ((o(i, j) - e(i, j)), d(i, j) - c(i, j))$$

in which the erosion and dilation operations are performed on the α trimmed blurred image, and the opening and closing operations are performed on the eroded and dilated images of the α trimmed blurred image.

The ATM edge detector, like the BMM edge detector, is unable to extract the weak gradients associated with certain mesoscale features [22]. This possibly could be because the definition of gray-scale dilation and erosion considers only the maximum and the minimum intensity pixels in a given neighborhood of a pixel. As a result, the dilation and erosion residual values are not sufficient for these edge detectors to pick up the weak gradients. For increased structuring element sizes, weak gradients are extracted, along with other spurious edge pixels which are difficult to isolate.

The cluster shade algorithm [7] presented earlier extracts most of the weak gradient valued pixels, along with the strong gradient valued pixels. This is due to the application of a texture-based algorithm in an application where multiple gradient values are vital for interpretation. The algorithm is very computation intensive [12].

We seek a low-level segmentation module that is simple in design and construction, despite making use of the texture information in the image. We anticipate that such a design would extract all the boundaries of the features irrespective of their gradient values. One of the possible methods of making use of texture information is to compute the first-order histogram in a neighborhood of a pixel.

B. Motivation and Scope

Previous morphological edge detectors are designed to work only in the image domain. Such designs ignore the vital information contained in the histogram of an (sub-) image. As a consequence, various weak gradient values pertaining to important features are missed in oceanographic IR images. We expect that a morphological edge detector that incorporates information from the image histogram will provide improved performance while being conceptually simple and computationally efficient. In Section IV, we propose new morphological operations defined over the histogram of a neighborhood of a pixel. The new morphological operations are limited to erosion and dilation only, and the morphological basis of these new operations is explained in the context of oceanographic images only.

IV. Histogram-Based Morphological Edge Detector

The histogram is a popular tool used in image processing and image analysis. It is used for edge detection, thresholding, texture feature extraction, and other related problems. Let H be the histogram of an image or subimage, let $g_0, g_1, \cdots, g_{l-1}$ be the gray levels for which the histogram is defined, and let $h(g_0), h(g_1), \cdots, h(g_{l-1})$ be the count values for those gray levels. Previously, researchers have designed image segmentation methods from the histogram using either global or local thresholding concepts. For instance, when a light object is present in dark background, the histogram may have twin peaks occurring at the intensities corresponding to the intensities of the object and background. A suitable threshold between the two peaks is selected to segment the object from the background [23]. When multiple objects are present in the background, a global histogram is of little use. However, a local histogram in the neighborhood of a pixel would exhibit twin peaks from which an object can be segmented from the background [24].

It is noted that the gray-scale dilation and erosion are the maximum and minimum of the image pixels spanned by the structuring element, respectively. The definitions of gray-scale morphology, in fact, make use of the histogram indirectly. This is explained using a structuring element S of height 0 in the following way: gray-scale dilation over the histogram is the maximum of $g_0, g_1, g_i, \cdots, g_{l-1}$ for which $h(g_i) \neq 0$. Similarly, the gray-scale erosion is the minimum of $g_0, g_1, g_i, \cdots, g_{l-1}$ for which $h(g_i) \neq 0$. The average of the image pixels is computed from the histogram. It is also noted that the BMM and ATM edge detectors extract edges using the gray-scale dilation and erosion operations. But these definitions consider only the maximum and minimum of the image pixel intensities in a given neighborhood. Thus, we infer that there is a clear distinction in theories between the histogram-based edge detectors and morphology-based edge detectors. The essential ideas in the former methods stem from the fact that the histogram taken near the boundaries exhibits twin peaks, while the latter methods mark a pixel as an edge pixel depending on the maximum and minimum intensity values of the pixels near the boundaries. We anticipate that morphological edge detectors that use the histogram in an effective way would reduce the gap between these two edge detection theories. In doing so, we will develop extensions to the definitions of morphological operations in the domain of the histogram, but not in the domain of the image. We anticipate that such extensions provide us new directions in the notion of morphology-based edge detectors, particularly in the context of oceanographic images.

Let a histogram H defined over gray levels $g_0, g_1, \cdots, g_{l-1}$ be computed using the image pixels spanned by the structuring element S centered at the coordinates (x, y). g_0 and g_{l-1} are the intensity of black and white pixels, respectively. Call the height of the histogram at these gray levels $h(g_0), h(g_1), \cdots, h(g_{l-1})$. Let the intensity of the pixel [at coordinates (x, y)], where the histogram is computed, be g_i. We define histogrammic dilation *h dilation* at a pixel (x, y) as

$$d_h(x, y) = \{g_j \mid h(g_j) = \max\,[h(g_i), h(g_{i+2}), \cdots, h(g_{l-1})] \text{ and } (i \leq j \leq l-1)\}.$$

Similarly, we define the histogrammic erosion *h erosion* as

$$e_h(x, y) = \{g_j \mid h(g_j) = \max\,[h(g_0), h(g_1), \cdots, h(g_i)] \text{ and } (0 \leq j \leq i)\}.$$

It is noted that both the d_h and e_h are defined in terms of peaks of the histogram on either side of the gray-level intensity g_i of the pixel. By defining these operations in this fashion, we make a noticeable deviation from the traditional dilation and erosion operations.

The value of e_h is the gray-level intensity g_e at which the histogram height is the maximum of all heights computed at gray-level intensities lower than the (average) gray-level intensity of the pixel. The value of d_h is the intensity g_d at which the histogram height is the maximum of all histogram heights computed at intensities greater than the (average) intensity of the pixel. In case a unique intensity $g_e(g_d)$ is not found, $g_e(g_d)$ that is closer to g_i is selected.

One of the motivations for using h dilation and h erosion is as follows. Fig. 1 is unusually free of clouds. Even though many cloud detection algorithms are available, none of them detects all cloud pixels [6]. Therefore, some cloud pixels will be present in the input image. We recall that the traditional dilation and erosion definitions consider only the extreme values in the neighborhood of a pixel. If a cloud pixel is one of the extreme values, then an edge detector based on traditional mathematical morphology will extract spurious edge pixels. We anticipate a reduction in the extraction of spurious edge pixels when we use the h-dilation and h-erosion operations.

A careful examination of these definitions indicates a strong link between the histogram-based and morphology-based edge detectors. For instance, consider a histogram computed in a neighborhood of a pixel near the boundary having (twin) peaks with the average intensity falling between the peaks. The histogram-based methods search for the *valleys and peaks* in the histogram, whereas the morphological methods (BMM and ATM) search for the *extreme* intensities that have nonzero histogram heights.

Fig. 2 is the new edge detector that makes use of the histogrammic dilation and erosion. The edge strength in the edge image at (x, y) is given by

$$\text{HMED}\,(x, y) = \min\,(f(x, y) - e_h(x, y), \; d_h(x, y) - f(x, y))$$

where $f(x, y)$ is the average intensity g_i at coordinate (x, y).

Thus, the edge magnitude values in the output image are computed in a similar fashion to that of the BMM and

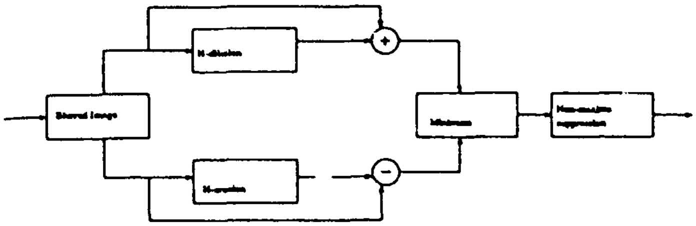

Fig. 2. Flowchart of HMED.

ATM edge detectors. Normally, an edge detector should generate edge pixels of width two in case of ideal step edges. However, this is not true for edge detectors that take input images which are blurred or smoothed versions of the original image. The HMED technique, when used with large structuring elements, produces significant nonzero edge strength of width more than one pixel. This is consistent with the fact that HMED blurs the original image. Usually, the true edge pixels get assigned higher edge strength than their neighbors. Normally, a suitable threshold is selected to extract the true edge pixels. However, HMED extracts the true edge pixels using a nonmaxima suppression technique.

Thus, we establish a computational framework that adapts the advantages of two edge detection theories. With such a computational framework, we show that HMED performs better than the BMM and ATM edge detectors.

A. Comments on HMED

The procedure HMED given in Fig. 2 takes a blurred image as input and produces an edge strength image in which nonmaxima suppression has to be performed.

It is noted that a new histogram is not computed from scratch at every pixel's neighborhood. The histogram of the adjacent neighborhood $(x, y + 1)$ is computed by using the histogram computed at pixel (x, y) as described in version 6 in [12].

The HMED algorithm presented here involves only parameters such as the size of the structuring element and nonmaxima suppression. No strict rules can be stated in this regard. For the images considered here, we present results that are produced with structuring element sizes 15×15, 17×17, 19×19, and 21×21.

There are at least two ways in which we can extract the true edges: computation of zero crossings and suppression of nonmaxima.

1) Let B denote a pixel in the blurred image, D the corresponding pixel in the H-dilated image, and E the corresponding pixel in the H-eroded image. Extract zero crossings in the following way. If (B-E) is less than (D-B), then assign $-$(B-E) as the value at that point in the edge strength image, else assign (D-B) as the value. Then a zero-crossing test has to be performed. The significance of a negative value is that the histogram is skewed to the negative side of the mean value. A positive value indicates that the histogram is skewed to the positive side of the mean value.

2) In case of nonmaxima suppression in the edge strength image, we suppress a pixel as a nonedge pixel if there exists a group of pixels whose value is much greater than the pixel to be suppressed [24].

B. Handling of Cloud Cover

The test image in Fig. 1 is unusually free of clouds. A typical oceanographic image contains cloud cover as well as attenuation due to water vapor. Thus, the low-level vision algorithms have to be designed to handle the cloud cover. One simple method to avoid the cloud pixels is to generate a cloud mask using a technique proposed in [6]. The cloud mask is a binary image that contains the values 0 or 1. A value 0 signifies that the pixel is part of a cloud and 1 signifies a noncloud pixel. In this application, cloud pixels are treated as follows.

1) A pixel in the IR image is considered a candidate edge pixel if and only if the cloud mask has value 1 at the same coordinate.

2) For a candidate edge pixel, the histogram is computed by considering only the noncloud pixels.

V. Implementation Results

The test data set consists of 12 satellite IR images of the North Atlantic. We present results from three. We processed the images with the BMM and ATM detectors using structuring elements of sizes 5×5, 7×7, 9×9, 11×11, and 13×13, while we used structuring element sizes of 13×13, 15×15, 17×17, 19×19, and 21×21 with the HMED detector. The ATM edge detector's α parameter was 3 in all cases. We do not know of any strict rules to govern the choice of the structuring element's size or the value of α.

Figs. 3 and 4 all show the results obtained with Fig. 1. Fig. 3 shows the results of applying the BMM edge detector with structuring elements of sizes 5×5, 7×7, 11×11, and 13×13. Increasing the structuring element's size results in finding more edges. Fig. 4 shows the results of applying the ATM detector with structuring elements of sizes 5×5, 9×9, 11×11, and 13×13. The results are slightly different, but again increasing the structuring element's size finds more edges. Figs. 5 and 6 are the h-dilated and h-eroded images of Fig. 1. Fig. 7 is the gradient image created by taking the minimum of the residuals. Fig. 8 shows the results of applying the HMED detector with window sizes 13×13, 15×15, 17×17, and 19×19. The HMED detector finds far fewer spurious edges, and increasing the window size seems to increase the continuity of the edges without finding many more.

Figs. 9 and 10 are also satellite images of the North Atlantic. Figs. 11, 12, and 13 show a comparative analysis of the three methods applied to the three images. In each case, the result with the structuring element judged to give the best performance is shown.

All three methods find the Gulf Stream's North Wall and boundaries of warm eddies for all structuring elements. These edges have high gradient values, so detection is relatively easy. The South Wall and boundaries of

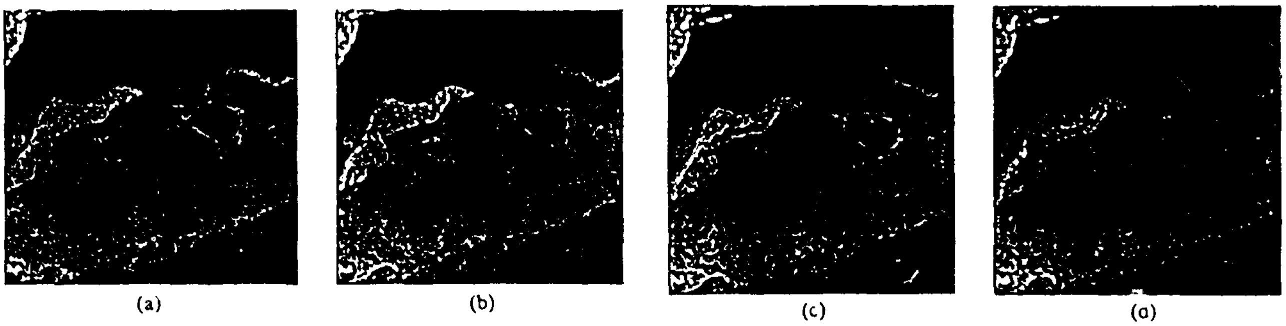

Fig. 3. Results of applying BMM on Fig. 1. (a) 5 × 5 structuring element, (b) 7 × 7 structuring element, (c) 11 × 11 structuring element, (d) 13 × 13 structuring element.

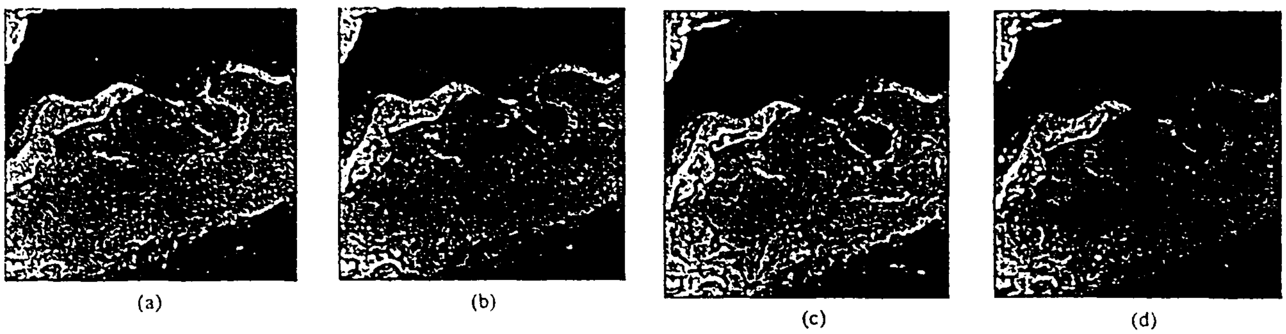

Fig. 4. Results of applying ATM on Fig. 1. (a) 5 × 5 structuring element, (b) 9 × 9 structuring element, (c) 11 × 11 structuring element, (d) 13 × 13 structuring element.

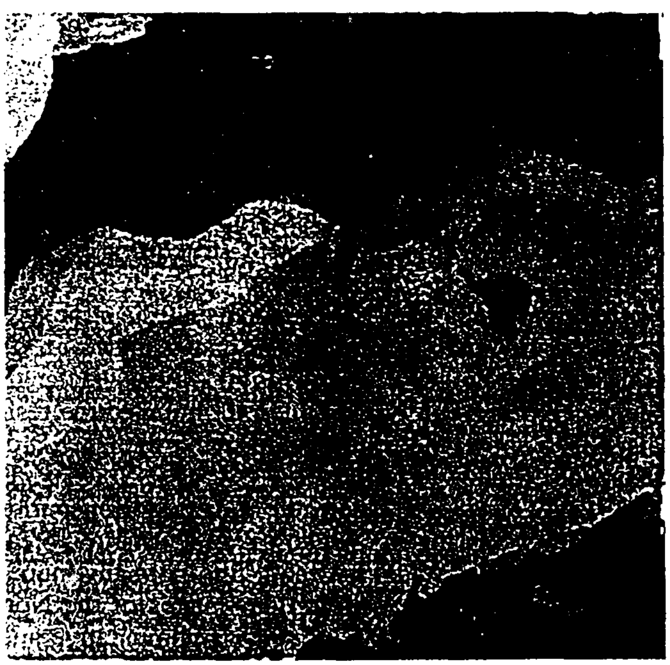

Fig. 5. *H*-dilated image of Fig. 1.

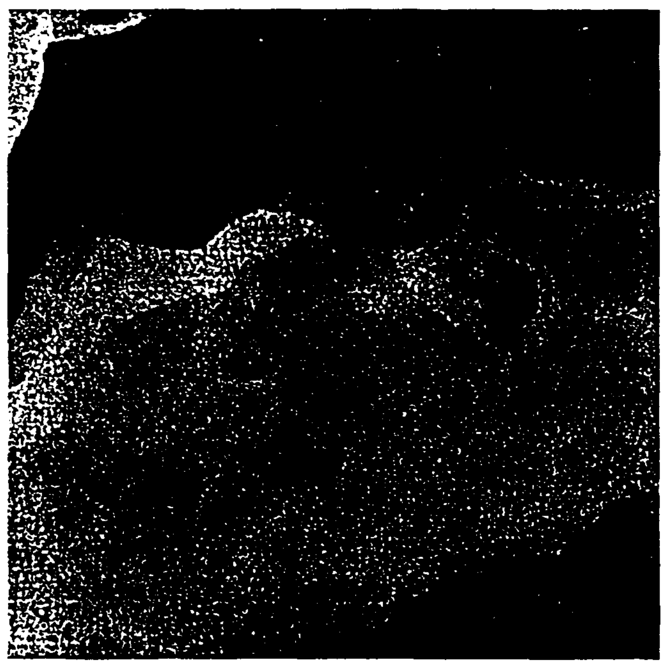

Fig. 6. *H*-eroded image of Fig. 1.

cold eddies are spatially distributed over 6–7 pixels with low gradient values. None of the detectors does as well in extracting these weak gradients as in finding the stronger ones when using small structuring elements. Increasing the size causes the BMM and ATM detectors to introduce many spurious edges. However, the HMED detector is able to extract these weak gradient values without introducing many spurious edge pixels.

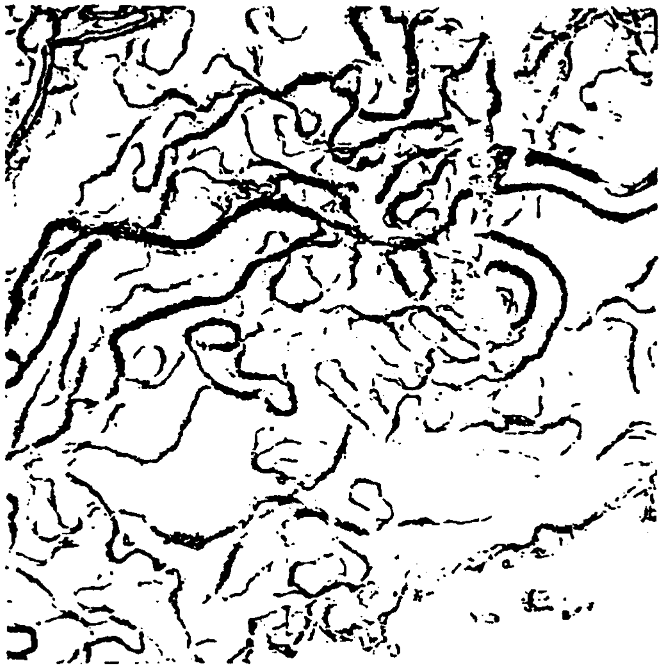

Fig. 7. Gradient image using Figs. 5 and 6.

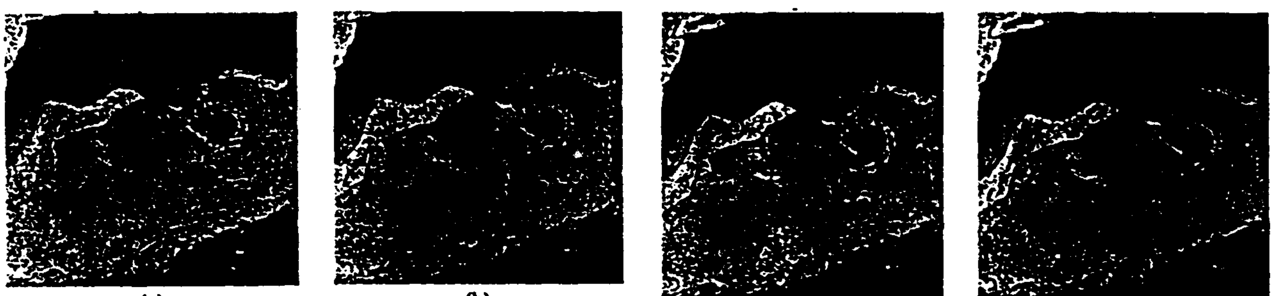

(a) (b) (c) (d)

Fig. 8. Results of applying HMED with various stucturing elements on Fig. 1. (a) 13 × 13 structuring element, (b) 15 × 15 structuring element, (c) 17 × 17 structuring element, (d) 19 × 19 structuring element.

Fig. 9. North Atlantic image obtained on April 10.

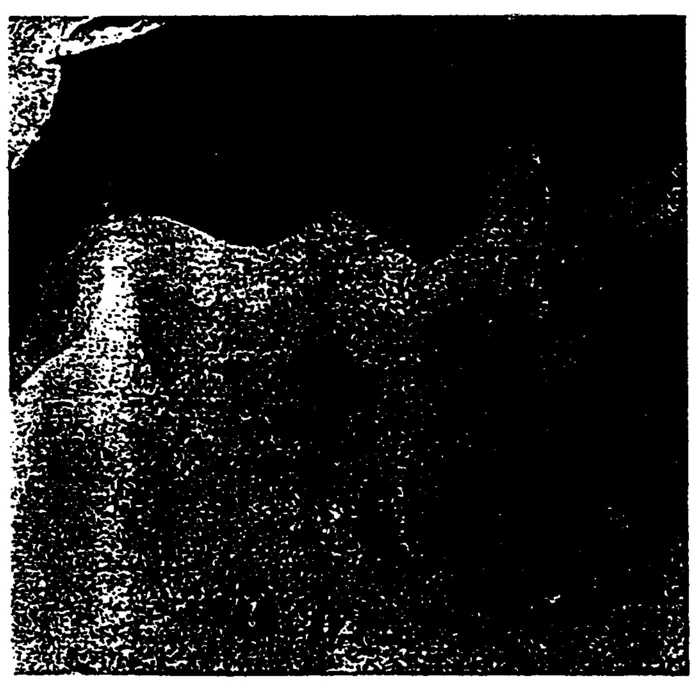

Fig. 10. North Atlantic image obtained on April 21.

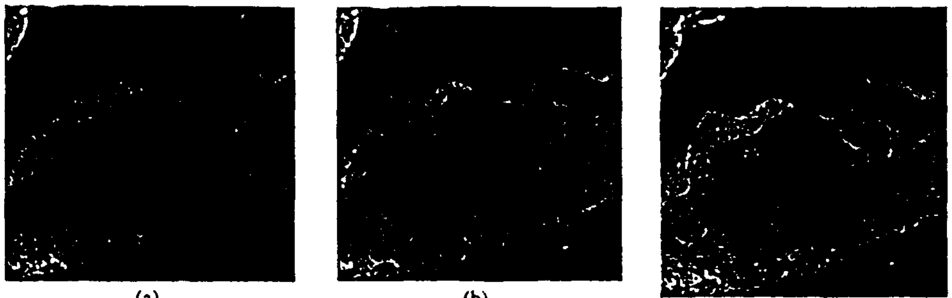

(a) (b) (c)

Fig. 11. Results of applying BMM, ATM, and HMED on Fig. 1. (a) BMM with 9 × 9 structuring element, (b) ATM with 7 × 7 structuring element, (c) HMED with 21 × 21 structuring element.

(a) (b) (c)

Fig. 12. Results of applying BMM, ATM, and HMED on Fig. 9. (a) BMM with 9 × 9 structuring element, (b) ATM with 7 × 7 structuring element, (c) HMED with 21 × 21 structuring element.

(a) (b) (c)

Fig. 13. Results of applying BMM, ATM, and HMED on Fig. 10. (a) BMM with 9 × 9 structuring element, (b) ATM with 7 × 7 structuring element, (c) HMED with 21 × 21 structuring element.

Again, HMED is able to extract the boundaries of the mesoscale features without introducing spurious edge pixels. We conclude that the HMED's better performance is due to the use of h dilation and h erosion.

References

[1] H. Stommel, *The Gulf Stream: A Physical and Dynamical Description*, 2nd ed. Berkeley, CA: Univ. California Press, 1965.

[2] F. C. Fuglister, "Cyclonic rings formed by the Gulf Stream 1965-1966," in *Studies in Physical Oceanography: A Tribute to George Wust on his 80th Birthday*, A. Gordon, Ed. New York: Gordon and Breach, 1972, pp. 137-168.

[3] P. L. Richardson, *Gulf Stream Rings, in Eddies in Marine Science*, editor: A. R. Robinson. Springer-Verlag, 1983, pp. 65-68.

[4] M. G. Thomason, "Knowledge-based analysis of satellite oceanographic images," *Int. J. Intell. Syst.*, vol. 4, pp. 143-154, 1989.

[5] M. Lybanon, J. D. McKendrick, R. E. Blake, J. R. B. Cockett, and M. G. Thomason, "A prototype knowledge-based system to aid the oceanographic image analyst," *Proc. SPIE, Vol. 635—Appl. of Artificial Intell. III*, pp. 203-206, 1987.

[6] S. Gallegos, J. Hawkins, and C. F. Cheng, "A new automated method of cloud masking for AVHRR full resolution data over the ocean," *J. Geophys. Res.: Oceans*, vol. 4, no. 5, pp. 8505-8516, 1993.

[7] R. J. Holyer and S. H. Peckinpaugh, "Edge detection applied to satellite imagery of the oceans," *IEEE Trans. Geosci. Remote Sensing*, vol. 27, pp. 45-56, Jan. 1989.

[8] J. Kittler and J. Illingworth, "Relaxation labeling algorithms—A review," *Image Vision Computing*, pp. 206-216, 1985.

[9] N. Krishnakumar, S. S. Iyengar, R. Holyer, and M. Lybanon, "Feature labeling in infrared oceanographic images," *Image Vision Computing*, vol. 8, no. 2, pp. 141-147, 1990.

[10] S. Krishnamurthy, S. S. Iyengar, R. Holyer, and M. Lybanon, "Topographic-based feature labeling of oceanographic images," *Pattern Recognition Lett.*, vol. 14, pp. 915-925, 1993.

[11] M. Lybanon and J. D. Thompson, "The role of expert systems in

ocean engineering,'' in *Conf. Proc., An Ocean Cooperative: Industry Government Academia*, 1990.

[12] S. Peckinpaugh, ''An improved method for computing gray-level cooccurrence matrix based texture measures,'' *CVGIP: Graphical Models and Image Processing*, vol. 53, no. 6, pp. 574–580, 1991.

[13] J.-F. Cayula and P. Cornillon, ''Edge detection applied to sea surface temperature fields,'' in *Proc. SPIE Tech. Symp. Opt. Eng. Photon. in Aerosp. Sensing*, 1990.

[14] G Matheron, *Random Sets and Integral Geometry*. New York: Wiley, 1975.

[15] J. Serra, *Image Analysis and Mathematical Morphological*. New York: Academic, 1982.

[16] R. Haralick, S. Sternberg, and X. Zhuang, ''Image analysis using mathematical morphology,'' *IEEE Trans. Pattern Anal. Machine Intell.*, vol. PAMI-9, July 1987.

[17] S. Pelag and A. Rosenfeld, ''A min-max medial axis transformation,'' *IEEE Trans. Pattern Anal. Machine Intell.*, pp. 206–210, 1981.

[18] S. Pelag, J. Naor, R. Hartley, and D. Avnir, ''Multiple resolution texture analysis and classification,'' *IEEE Trans. Pattern Anal. Machine Intell.*, pp 518–523, 1984.

[19] M. Werman and S. Pelag, ''Min-max operators in texture analysis,'' *IEEE Trans. Pattern Anal. Machine Intell.*, pp. 730–733, Nov. 1985.

[20] J. Lee, R. Haralick, and L. Shapiro, ''Morphologic edge detection,'' *IEEE J. Robotics Automation*, vol. RA-3, Apr. 1987.

[21] R. Feehs and G. Arce, ''Multidimensional edge detection,'' *Proc. SPIE, Visual Commun. Image Processing II*, vol. 845, pp. 285–292, 1987.

[22] S. Krishnamurthy, S. S. Iyengar, R. Holyer, and M. Lybanon, ''Morphological edge detection for oceanographic images,'' *Interdisciplinary Comput. Vision: Appl. and Changing Needs, SPIE Proc.*, vol. 2103, 1993.

[23] P K. Sahoo, S. Soltani, and A. K. C. Wong, ''A survey of thresholding techniques,'' *CVGIP*, pp. 233–260, 1988.

[24] A. Rosenfeld and A. Kak, *Digital Picture Processing*. New York: Academic, 1982.

Sankar Krishnamurthy received the B.S. degree from the Regional Institute of Technology, India, in 1986, and two M.S. degrees from LSU, one in engineering science and the other in computer science.

From 1989 to 1991 he was a Research Assistant at the Remote Sensing and Image Processing Laboratory, LSU. Currently, he is a Research Assistant at the Robotics Research Laboratory at LSU, where he is also studying towards the Ph.D. degree in computer science. He is also working with the Research Group at Naval Research Laboratory, Department of the Navy, Stennis Space Center, MS, to develop image analysis algorithms for oceanographic data. His research interests are in computer vision, computer graphics, visualization, and multimedia.

S. Sitharama Iyengar (M'88–SM'90) received the Ph.D. degree from Mississippi State University in 1974.

He is the Chairman of the Computer Science Department and Professor of Computer Science at Louisiana State University. He has directed LSU's Robotics Research Laboratory since its inception in 1986. He has been actively involved with research in high-performance algorithms and data structures since 1974, and has directed more than 18 Ph.D. dissertations at LSU. He has served as principal investigator on research projects supported by the Office of Naval Research, the National Aeronautics and Space Administration, the National Science Foundation/Laser Program, the California Institute of Technology's Jet Propulsion Laboratory, the Department of the Navy's NRL, the Department of Energy (through Oak Ridge National Laboratory, TN), the LEQFS-Board of Regents, and Apple Computers. He has edited a two-volume tutorial on autonomous mobile robots, and has edited two other books and more than 150 publications, including 90 archival journal papers in areas of high-performance parallel and distributed algorithms and data structures for image processing and pattern recognition, autonomous navigation, and distributed sensor networks. He was a Visiting Professor (Fellow) at JPL, the Oak Ridge National Laboratory, and the Indian Institute of Science. He is also an Association for Computing Machinery National Lecturer, a Series Editor for *Neuro Computing of Complex Systems*, and Area Editor for the *Journal of Computer Science and Information*. He has served as Guest Editor for the IEEE TRANSACTIONS ON SOFTWARE ENGINEERING (1988), IEEE COMPUTER magazine (1989), IEEE TRANSACTIONS ON SYSTEMS, MAN, AND CYBERNETICS, IEEE TRANSACTIONS ON KNOWLEDGE AND DATA ENGINEERING, and the *Journal of Computers and Electrical Engineering*.

Dr. Iyengar was awarded the Phi Delta Kappa Research Award of Distinction at LSU in 1989, won the Best Teacher Award in 1978, and received the Williams Evans Fellowship from the University of Otago, New Zealand, in 1991.

Ronald J. Holyer received the B.A. degree in physics and mathematics from Augustana College in 1964, the M.S. degree in physics from the South Dakota School of Mines and Technology in 1966, and the Ph.D. degree in geology from the University of South Carolina in 1989.

He is Head of the Computer Sciences and Physics Section of the Remote Sensing Applications Branch of the Naval Research Laboratory at Stennis Space Center, MS. His interests are image processing, pattern recognition, and automated image interpretation.

Matthew Lybanon received the B.S. and M.S. degrees in physics from the Georgia Institute of Technology in 1960 and 1962, respectively.

He is currently a member of the Remote Sensing Applications Branch of the Naval Research Laboratory, Stennis Space Center, MS. His current research interests include expert systems, generalized nonlinear least squares methods, genetic algorithms, image processing, mathematical morphology, and applications of those topics to the extraction of information on ocean dynamics and sea ice from satellite observations.